

Infrared Diode Laser Spectroscopy of the SiF Radical

KEIICHI TANAKA, YASUNOBU AKIYAMA, AND TAKEHIKO TANAKA

*Department of Chemistry, Faculty of Science, Kyushu University 33,
Hakozaki, Higashiku, Fukuoka 812, Japan*

The vibration-rotation spectrum of the SiF radical produced in a glow discharge of silicon tetrafluoride (SiF₄) was observed using an infrared diode laser spectrometer. The SiF lines were discriminated from much stronger SiF₂ lines by the discharge current modulation and Zeeman modulation techniques. Twelve and 15 lines belonging to the ²Π_{1/2} and ²Π_{3/2} spin states, respectively, were identified for the fundamental band in the ground electronic state. Most of the lines in the ²Π_{1/2} state were observed with splitting due to the Δ-type doubling.

Precise molecular constants for the *v* = 1 state, including the rotational, centrifugal distortion, and spin-orbit coupling constants, were obtained from the least-squares analysis, in which the ground state constants were constrained as determined by microwave spectroscopy. The fundamental band origin thus obtained is 847.7205 ± 0.0005 cm⁻¹, where the uncertainty corresponds to three standard deviations. The equilibrium bond length *r*_e is derived as 1.601018 ± 0.000003 Å from the equilibrium rotational constant, *B*_e = 0.581241 ± 0.000002 cm⁻¹. © 1989 Academic Press, Inc.

INTRODUCTION

Spectroscopy of the SiF radical has currently been attracting much interest in connection with plasma etching and sputtering processes. Walkup *et al.* (1) detected the SiF radical produced in the CF₄ + O₂ plasma reacting with a silicon substrate, monitoring the A²Σ⁺ → X²Π emission by laser-induced fluorescence (LIF). The electronic spectrum of SiF has been studied extensively as summarized by Huber and Herzberg (2). Appelblad *et al.* (3) and Martin and Merer (4) have reported rotational analyses of the C²Δ → X²Π and a⁴Σ → X²Π transitions, respectively. Many transitions in the UV and VUV regions, including those involving Rydberg states, have been rotationally analyzed by Houbrechts *et al.* (5-8). These rotational analyses gave the molecular constants for various vibrational states in the ground electronic state as well as those in the excited states. The optical studies have shown that the ground electronic state of SiF is a regular ²Π state with a ²Π_{3/2}-²Π_{1/2} separation of about 162 cm⁻¹ (3, 4).

Although the LIF method allows us to observe the emission spectrum of SiF, the detection of the SiF spectrum within the ground electronic state is also highly desirable in view of recent industrial interest. However, few spectroscopic studies within the ground state have been reported. Recently, Tanimoto *et al.* (9) observed the microwave spectrum of SiF in the ²Π_{1/2} and ²Π_{3/2} states and obtained precise molecular constants in the ground vibrational state including hyperfine interaction constants.

In the present paper, we report infrared diode laser spectroscopy of the SiF radical generated in a glow discharge of silicon tetrafluoride (SiF₄). The spectrum was recorded

by the discharge modulation method using a multireflection absorption cell. The Zeeman modulation technique as well as the discharge modulation method was applied to discriminate the SiF radical from other species in the plasma. The infrared spectrum of the SiF⁺ ion was also observed in the negative glow of the SiF₄ discharge using a hollow cathode absorption cell. The detection of the SiF⁺ ion has been reported separately (10).

EXPERIMENTAL DETAILS

Figure 1 illustrates the infrared diode laser spectrometer used for the measurement, which was newly constructed at Kyushu University. Infrared emission from a Spectra-Physics diode laser (SP5615) was collimated into a parallel beam by a 90° off-axis parabola of 3.175 cm focal length and passed through a 50-cm monochromator, which selected a single mode from multimode oscillation. The infrared light was then split into three beams by ZnSe plates. Two of the beams, which were for the wavenumber calibration, were passed one through a reference gas cell and another through a vacuum-spaced etalon. The etalon consisted of two Ge menisci spaced by a 25-cm quartz tube to form a confocal resonator. The free spectral range of the etalon was calibrated to be $0.009979 \pm 0.000003 \text{ cm}^{-1}$ using the lines of OCS (11) as the standard. The third beam was introduced into an absorption cell for the detection of short-lived species. Each beam was detected by a HgCdTe detector.

The absorption cell used for the present measurement is shown in Fig. 2. It consisted of a 106-cm-long Pyrex glass tube with 50 mm diameter in its central 85-cm part. Near the ends of the tube, a pair of 5-cm-long 45-mm i.d. stainless-steel cylinders were placed, separated by about 65 cm, as electrodes for discharge. Ac high voltage of about 1 kHz generated by a 1.4-kW amplifier and stepped up by a transformer (1:30) was applied between the electrodes. Glow discharge occurred twice in each cycle of the ac

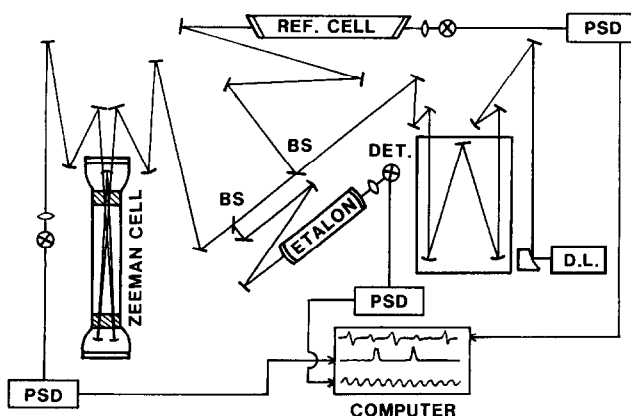


FIG. 1. Schematic diagram of the diode laser spectrometer. Infrared light emitted from a diode laser (DL) is split into three by ZnSe beam splitters (BS) after passing through a 50-cm monochromator. The beams are led to a reference cell and an etalon, for wavenumber calibration, and an absorption cell, and focused onto HgCdTe detectors. The signal was phase-sensitively detected (PSD) with reference to discharge or Zeeman modulation and accumulated in a microcomputer.

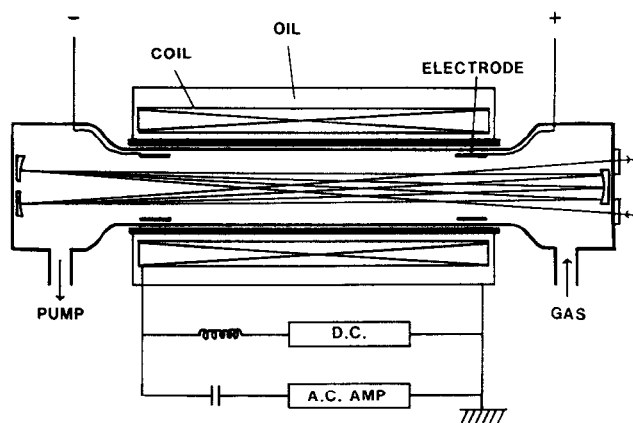


FIG. 2. Absorption cell used for Zeeman modulation. A 1-kHz ac magnetic field up to 500 G peak-to-peak superposed on a dc field is generated by the solenoid coil wound outside the cell and immersed in an oil tank. A dc high voltage of about 100 mA is applied between electrodes to produce a glow discharge. Three concave mirrors form a White-type multireflection optical path.

voltage, in alternating directions, and the signal was detected by a phase sensitive detector (PSD) operating at twice the frequency of the ac high voltage. The discharge cell was incorporated with a White-type multireflection optical path formed by three concave mirrors of 50 cm focal length. The laser beam traveled ten round trips, yielding an effective path length of 20 m.

A solenoid coil was placed outside the cell for the detection of Zeeman sensitive lines. It consisted of resin-coated copper wire of $2 \times 3 \text{ mm}^2$ cross section wound in six layers around an 80-cm-long fiber-reinforced-plastic tube with a diameter of 66 mm. A 1-kHz alternating current was fed to the solenoid through a capacitor, which was in series resonance with the coil, to produce an axial ac magnetic field up to 500 G peak-to-peak. A direct current was simultaneously fed to the solenoid through a choke coil to enhance modulation efficiency. When Zeeman modulation was used, the radical was generated by a dc glow discharge, and the PSD was operated at the same frequency as that of the magnetic field ($1f$) or twice that ($2f$). The coil was immersed in an oil tank cooled by circulating water.

The absorption cell was evacuated by a high-speed mechanical booster pump backed up by a rotary pump. The observed wavenumbers were calibrated using the lines of OCS (11) as reference, and a vacuum-spaced etalon as an interpolation device. The PSD outputs for the SiF lines, reference lines, and etalon fringes were accumulated in a microcomputer.

OBSERVED SPECTRA

The SiF radical was produced directly in the absorption cell in the glow discharge of SiF₄. Pure SiF₄ gas was used and the optimum pressure at the inlet to the absorption cell was about 200 mTorr. Mixing of He or N₂ decreased the SiF signal intensity. Addition of H₂ led to production of SiHF₃ in an appreciable amount and almost total

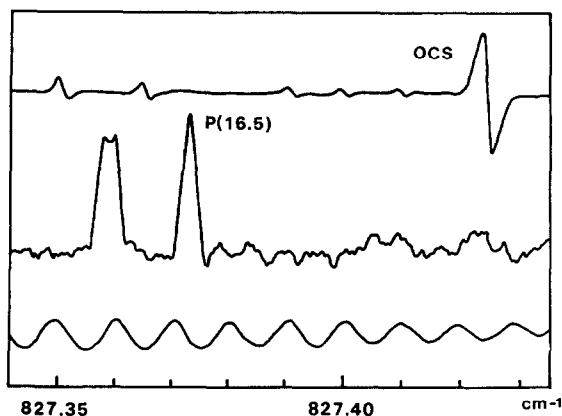


FIG. 3. Observed spectrum of the $P(16.5)$ lines for the ${}^2\Pi_{1/2}$ (left) and ${}^2\Pi_{3/2}$ (right) spin states recorded by discharge modulation with 427-Hz ac current of 190 mA peak-to-peak. Splitting of the ${}^2\Pi_{1/2}$ state line due to the Λ -type doubling is observed. The spectra of OCS (top) and etalon fringes (bottom) were used for wavenumber calibration.

loss of the SiF signal. The optimum discharge current was about 190 mA peak-to-peak. The optimum frequency of the ac voltage for discharge was 427 Hz. Higher frequencies than 1 kHz resulted in rather unstable discharge.

Twelve transitions in the ${}^2\Pi_{1/2}$ spin state (P and R branch lines) and 15 transitions in the ${}^2\Pi_{3/2}$ spin state (P , Q , and R branch lines) for the fundamental band were observed in the frequency range of $813\sim 876\text{ cm}^{-1}$. Most of the transitions in the ${}^2\Pi_{1/2}$ state were observed as doublets which were split by about 0.004 cm^{-1} due to Λ -type doubling. Observation of the SiF lines was sometimes obstructed by the intense ν_1 and ν_3 bands of SiF_2 , which was produced simultaneously in the cell by the glow discharge of SiF_4 . However, the SiF lines were easily discriminated from the crowded SiF_2 lines because the two kinds of lines behaved differently when the frequency of the discharge modulation or the phase of the PSD was changed. As the frequency of the discharge modulation was decreased, the SiF_2 lines got stronger, indicating a longer lifetime of SiF_2 . Figure 3 shows a typical trace of the observed lines recorded by discharge modulation. The two signals are assigned to the $P(16.5)$ lines for the ${}^2\Pi_{1/2}$ and ${}^2\Pi_{3/2}$ spin states; the line for the ${}^2\Pi_{1/2}$ state is split slightly due to the Λ -type doubling. The signal-to-noise ratio was about 20 for $P(16.5)$, the strongest of the observed lines. The width of the observed lines was about 70 MHz FWHM. For comparison, the calculated Doppler widths are 53 and 75 MHz FWHM at 400 and 800 K, respectively, and the expected frequency jitter of the light source is about 15 MHz. The observed SiF lines in the both spin states are listed in Table I with their assignments. The accuracy of the measured wavenumbers is about 0.0005 cm^{-1} .

The Q -branch lines in the ${}^2\Pi_{3/2}$ state were hardly observed by discharge modulation because of the serious overlap with intense SiF_2 lines. However, we successfully detected them by the Zeeman modulation method. The radical was produced by a 50-mA dc discharge in the SiF_4 gas, and the signals were modulated with a 911-Hz ac magnetic field of 400 G peak-to-peak superposed on a dc field of 200 G. Figure 4 illustrates the

TABLE I

Observed Diode Laser Spectrum of the SiF Radical^a

Transition	Obs.	O-C ^b	Transition	Obs.	O-C ^b
² Π _{1/2} P(26.5) e,f	813.803 4	2	² Π _{3/2} P(26.5)	813.702 3	-6
P(16.5) e	827.358 7	2	P(16.5)	827.373 0	-7
f	827.360 3	-7	P(13.5)	831.288 0	-3
P(13.5) e	831.241 2	2	P(10.5)	835.115 5	0
f	831.242 8	-8	P(6.5)	840.081 7	6
P(10.5) e	835.037 4	1	Q(1.5)	847.792 2	-4
f	835.039 7	-4	Q(2.5)	847.766 6	-8 c
P(6.5) e	839.963 8	2	Q(3.5)	847.731 5	-6 c
f	839.966 4	-2	R(7.5) f	857.277 2	3
R(3.5) f	852.701 8	0	e	857.037 7	-3
e	852.705 0	1	R(8.5)	858.341 7	-3
R(7.5) f	857.034 2	-8 c	R(11.5)	861.475 2	4
e	857.037 7	-3	R(12.5)	862.499 0	7
R(12.5) f	862.223 0	-5	R(16.5) f	866.488 2	5
e	862.226 5	0	e	866.192 9	-1
R(15.5) f	865.213 4	-4	R(21.5) f	870.914 1	-11 c
e	865.217 1	3 c	e	870.918 0	-1
R(16.5) f	866.189 3	-7	R(26.5) f	875.378 2	-4
e	866.192 9	-1	e	875.380 7	-6 c

a) In cm⁻¹ units.b) Observed minus calculated wavenumber in 10⁻⁴ cm⁻¹.

c) Less weighted in the analysis.

$Q(1.5) \sim Q(3.5)$ lines of the ²Π_{3/2} state recorded by Zeeman modulation with the PSD detection at twice the modulation frequency ($2f$ detection). A characteristic feature of the Q -branch lines, i.e., a rapid decrease of the line intensity with the J value, is clearly seen in Fig. 4, and the $Q(4.5)$ line was probably too weak to be observed. The line widths of the observed Q -branch lines show that the magnetic field was sufficient for modulation of the $Q(1.5) \sim Q(3.5)$ lines. The detection of the Q -branch lines by Zeeman modulation definitely shows that the carrier of the present spectrum is a paramagnetic species. However, no P - or R -branch lines of the ²Π_{3/2} state were observed by Zeeman modulation, probably because transitions with high J values are rather insensitive to magnetic fields. No lines of the ²Π_{1/2} state were detected by Zeeman modulation because the orbital and spin magnetic moments cancel each other in the ²Π_{1/2} state. The SiF₂ lines were almost completely suppressed in the case of Zeeman modulation.

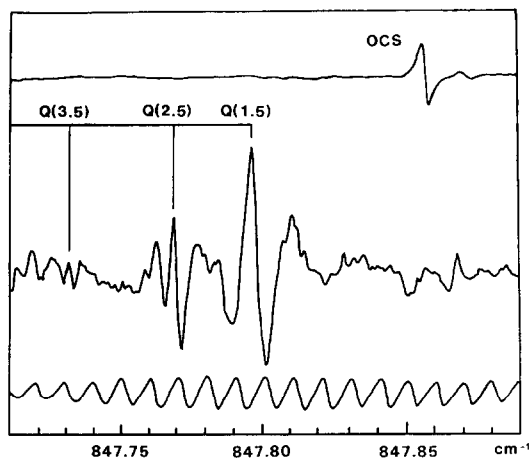


FIG. 4. The $Q(1.5) \sim Q(3.5)$ lines of the ${}^2\Pi_{3/2}$ state observed by Zeeman modulation with a 911-Hz ac magnetic field. The spectrum was recorded with PSD operated at twice the modulation frequency ($2f$).

No lines of the hot band or of the isotopic species were observed with the present positive column type cell. The line intensity of the SiF radical was not apparently enhanced by the use of a hollow cathode type cell, which we employed for the detection of the SiF⁺ ion in the SiF₄ plasma (10).

ANALYSIS

The Hamiltonian for a diatomic molecule in the ${}^2\Pi$ electronic state was originally derived by Hill and Van Vleck (12) and has been extended by many authors (13–18). In the present study, we use an effective Hamiltonian similar to that given in Hirota's textbook (19). Its matrix elements are written using a basis set consisting of the Hund's case (*a*) functions,

$$|{}^2\Pi_{\Omega}, J, \pm\rangle = \{ |J, \Omega, S, \Sigma, \Lambda\rangle \pm (-1)^{J-S} |J, -\Omega, S, -\Sigma, -\Lambda\rangle \} / 2^{1/2}, \quad (1)$$

which are taken to have the parity \pm . They correspond to the *e* and *f* labels for the Λ -doublet components first introduced by Kopp and Hougen (20) and recommended by Brown *et al.* (21) as follows: $|{}^2\Pi_{\Omega}, J, +\rangle$ and $|{}^2\Pi_{\Omega}, J, -\rangle$ correspond to *e* and *f*, respectively, when $J - \frac{1}{2} = \text{even}$, and the reverse when $J - \frac{1}{2} = \text{odd}$. The matrix elements of the effective Hamiltonian for the vibrational state *v* are

$$\begin{aligned} \langle {}^2\Pi_{1/2}, J, \pm | H_v | {}^2\Pi_{1/2}, J, \pm \rangle &= -A_v/2 - \gamma_v + o_v^* + (p_v^* + q_v^*)/2 + D_v \\ &+ (B_v - A_{Dv}/2 - D_v + q_v^*/2)X^2 - D_v X^4 \mp (-1)^{J-1/2} (q_v + p_v/2)X, \quad (2) \end{aligned}$$

$$\begin{aligned} \langle {}^2\Pi_{3/2}, J, \pm | H_v | {}^2\Pi_{3/2}, J, \pm \rangle \\ = A_v/2 + q_v^*/2 + 3D_v + (B_v + A_{Dv}/2 + 3D_v + q_v^*/2)(X^2 - 2) - D_v X^4, \quad (3) \end{aligned}$$

and

$$\begin{aligned} \langle {}^2\Pi_{3/2}, J, \pm | H_v | {}^2\Pi_{1/2}, J, \pm \rangle &= -\{ B_v - \gamma_v/2 + p_v^*/4 + q_v^*/2 \\ &- 2D_v(X^2 - 1) \mp (-1)^{J-1/2} (q_v/2)X \} (X^2 - 1)^{1/2}, \quad (4) \end{aligned}$$

where $X = J + \frac{1}{2}$ and the standard notation for the molecular constants is adopted. The A_{Dv} constant represents the centrifugal distortion correction to the spin-orbit coupling constant A_v , and the γ_v constant the spin-rotation interaction. The p_v , q_v , o_v^* , p_v^* , and q_v^* constants account for the effect of interactions with the ${}^2\Sigma^+$ and ${}^2\Sigma^-$ electronic states through the coupling of the electronic orbital angular momentum with the electron spin and rotational angular momenta. The p_v and q_v constants give rise to the Λ -doubling. Interactions with the Δ electronic states may contribute additional terms similar to the o_v^* , p_v^* , and q_v^* terms. The A_{Dv} and γ_v constants cannot be determined separately as pointed out by Brown and Watson (22). As discussed by Endo *et al.* (23), B_v cannot be separated from q_v^* , nor A_{Dv} from p_v^* . Also, A_v is not separable from o_v^* . Therefore, we use the effective constants

$$A_v^{\text{eff}} = A_v + \gamma_v - (o_v^* + p_v^*/2), \quad (5-1)$$

$$B_v^{\text{eff}} = B_v + q_v^*/2, \quad (5-2)$$

$$A_{Dv}^{\text{eff}} = A_{Dv} - (2\gamma_v - p_v^*)/(\lambda_v - 2), \quad (5-3)$$

where $\lambda_v = A_v/B_v$, i.e., the spin-orbit coupling constant divided by the rotational constant. In practice, we fixed o_v^* , p_v^* , q_v^* , and γ_v to zero in the analysis. Because the observed spectrum showed no hyperfine splittings due to the fluorine nucleus, the hyperfine interaction was ignored in the present analysis.

The observed wavenumbers were least-squares fitted. The molecular constants in the ground vibrational state were fixed at the values determined by microwave spectroscopy (9) and the spin-orbit coupling constant in the ground state at the value obtained from optical spectroscopy (4). As the Λ -type doubling in the ${}^2\Pi_{3/2}$ state was not resolved, the q_v constant in the $v = 1$ state could not be determined, and was assumed to have the same value as that in the ground state. The average of the calculated frequencies for the components of the Λ -type doublet was fitted to the observed frequency. It is noted that q_v should be regarded as an effective constant which involves the higher-order contribution of the p_J term (24), since no Λ -type splittings were resolved for the ${}^2\Pi_{3/2}$ state in the ground-state microwave spectrum. The linear combinations, $p_v + 2q_v$ and q_v , were optimized in the least-squares analysis instead of p_v and q_v themselves, as was done in the analysis of the microwave spectrum (9). The signs of the p_v and q_v constants were assumed to be negative according to the result of the microwave study (9).

The optimized molecular constants are listed in Table II along with the ground-state constants constrained in the least-squares fit. The standard deviation of the fit was about 0.0004 cm^{-1} , consistent with the experimental accuracy.

DISCUSSION

The present analysis of the diode laser spectrum gave the molecular constants of the $v = 1$ state and an accurate value of the fundamental band origin $\nu_0 = 847.72048 \pm 0.00051 \text{ cm}^{-1}$. From the constants in Table II, equilibrium molecular constants are derived as shown in Table III and compared with the previous results by Martin and Merer (4). The agreement is satisfactory for the rotational constant B_e and vibration rotation constant α_e ; these two constants were evaluated from the effective rotational

TABLE II
Molecular Constants of the SiF Radical^a

Const.	$\nu = 0^c$	$\nu = 1$	
B^{eff}	0.578 7428 8 (21)	0.573 745 7 (38)	cm^{-1}
D	1.063 4 (43)	1.063 6 (48)	10^{-6}cm^{-1}
$A_0^{eff\ b}$	1.087 8 (28)	1.030 (24)	10^{-4}cm^{-1}
A^{eff}	161.88(1) ^d	162.044 44 (73)	cm^{-1}
$p+2q$	-3.008 4 (57)	-3.021 (87)	10^{-3}cm^{-1}
q	-0.042 0 (97)	-0.042 0 ^e	10^{-3}cm^{-1}
ν_0	847.720 48 (51)		cm^{-1}

- a) The figures in parentheses are three standard deviations in units of the last digit.
 b) A_0^{eff} corresponds to $2A_J$ in Ref. (9).
 c) Fixed. Ref. (9).
 d) Fixed. Ref. (4).
 e) Fixed to the ground state value.

constants, B_0^{eff} and B_1^{eff} , ignoring the q_v^* term in Eq. (5-2). The harmonic vibrational frequency, $\omega_e = 857.20 \pm 0.10 \text{ cm}^{-1}$, also agrees well with the reported value. The hot band was not observed in the present measurement, and the anharmonic constant $\omega_e x_e$ was assumed to be $4.74 \pm 0.05 \text{ cm}^{-1}$ as given by Appelblad *et al.* (3). The uncertainty of the harmonic frequency is due primarily to that in the assumed $\omega_e x_e$. The equilibrium bond length was determined to be $1.601018 \pm 0.000003 \text{ \AA}$, where the uncertainty of Planck constant was also taken into account. This value is about

TABLE III
Equilibrium Constants of the SiF Radical^a

Const.	Present	Ref. (3)	
B_e	0.581 241 5 (19)	0.581 38 (15)	cm^{-1}
α_e	0.004 997 2 (38)	0.004 90 (12)	cm^{-1}
ω_e	857.20 (10)	857.20 (15)	cm^{-1}
$\omega_e x_e$	4.74 (5) ^b	4.74 (5)	cm^{-1}
r_e	1.601 018 (3) ^c	1.600 8	\AA

- a) The figures in the parentheses are three standard deviations in units of the last digits.
 b) Assumed.
 c) The uncertainty in Planck constant is included.

0.011 Å larger than the equilibrium SiF bond length, 1.5901 ± 0.0001 Å, in SiF₂ (25). The centrifugal distortion constant $D_e = 1.0690 \times 10^{-6}$ cm⁻¹ calculated from the relation $D_e = 4B_e^3/\omega_e^2$ is consistent with the observed value (1.0633 ± 0.0068) $\times 10^{-6}$ cm⁻¹.

The Zeeman energy of the SiF radical is expressed as

$$\Delta E = -g_J \mu_B M_J B_Z, \quad (6)$$

where g_J is the g factor, μ_B the Bohr magneton, and M_J the component of the angular momentum along the external magnetic field B_Z . The g factor in the intermediate case ($a \sim b$) is given by (15)

$$g_J = -\{g_L + (g_S/4) \pm [(g_L + g_S)(\lambda - 2)/2 - g_S(J - \frac{1}{2})(J + \frac{3}{2})] / [4(J + \frac{1}{2})^2 + \lambda(\lambda - 4)]^{1/2}\} / [J(J + 1)], \quad (7)$$

where g_L and g_S are the g factors for the orbital and spin magnetic moments, respectively, and the \pm signs refer to the $^2\Pi_{3/2}$ and $^2\Pi_{1/2}$ spin states.

Since the spin-orbit coupling constant is much larger than the rotational constant ($\lambda = 279.7 \gg 1$), the g_J factor may be approximated, for the $^2\Pi_{3/2}$ state, by

$$g_J = -3/[J(J + 1)] + 2\{1 - 3/[4J(J + 1)]\}/(\lambda - 2), \quad (8-1)$$

and, for the $^2\Pi_{1/2}$ state, by

$$g_J = -2\{1 - 3/[4J(J + 1)]\}/(\lambda - 2), \quad (8-2)$$

where we adopted a reasonable assumption that $g_L = 1$ and $g_S = 2$.

The Zeeman pattern for the Q -branch lines is simple, with only two resolved components corresponding to $\Delta M_J = +1$ and $\Delta M_J = -1$. The g_J factors for the $J = 1.5$, 2.5, and 3.5 levels of the $^2\Pi_{3/2}$ state are calculated from the above formula to be -0.7943 , -0.3363 , and -0.1837 . The Zeeman shifts of the $\Delta M_J = \pm 1$ components of the $Q(1.5)$, $Q(2.5)$, and $Q(3.5)$ lines are ± 223 MHz, ± 95 MHz, and ± 52 MHz, when the magnetic field is 200 G. The calculated shifts explain fairly well the observed Zeeman-modulated line profiles of the Q -branch transitions, where the observed Doppler width of typically 70 MHz FWHM is taken into account. The Zeeman shifts observed with dc magnetic fields up to 500 G are also consistent with the above calculated g factors, e.g., the g_J factor observed for the $J = 1.5$ level was -0.80 ± 0.03 .

As for the $^2\Pi_{1/2}$ state, the g_J factors are small, e.g., they are -0.00683 and -0.00695 for the $J = 3.5$ and 4.5 levels, respectively. The Zeeman shift for the $R(3.5)$, $M_J = 4.5 \leftarrow 3.5$ transition is 2.08 MHz/200 G, which is too small to cause efficient Zeeman modulation with the available magnetic field.

The laser source was sensitive to stray magnetic fields and sometimes suffered from spurious frequency modulation synchronous with the Zeeman modulation, resulting in a noisy spectrum. We found that the $2f$ detection worked as well as the $1f$ detection, giving a slightly better signal-to-noise ratio.

In spite of a careful search, no hot-band lines were observed. This fact together with the observed linewidth may indicate that the gas temperature in the discharge was not extremely high; it was perhaps around 400 K. The lifetime of SiF in the plasma was estimated to be about 1 msec, because the optimum frequency for the discharge mod-

ulation was about 500 Hz. The concentration of SiF obtained was probably much lower than that of the CF radical attained in the discharge of CF₃I (26), for which infrared power absorption of about 10% has been reported. The main product in the discharge of pure SiF₄ is SiF₂. However, several lines which may be attributed to a short-lived species other than SiF and SiF₂ were also observed. The species has a lifetime similar to that of SiF, but the optimum phase of PSD, using discharge modulation, was different from that for SiF. A possible candidate for the carrier of the unidentified spectrum is the SiF₃ radical (27), of which the ν_1 band (SiF stretch) is expected to be in this region.

ACKNOWLEDGMENTS

We thank Professor E. Hirota, Dr. K. Kawaguchi and Dr. C. Yamada of IMS for encouragement throughout the present study. This work was supported by the Grant-in-Aid for Scientific Research on Priority Areas (63606006). Calculations for the present study were carried out at the Computer Center of Kyushu University.

RECEIVED: March 27, 1989

REFERENCES

1. R. WALKUP, PH. AVOURIS, R. W. DREYFUS, J. M. JASINSKI, AND G. S. SELWYN, *Appl. Phys. Lett.* **45**, 372-374 (1984).
2. K. P. HUBER AND G. HERZBERG, "Molecular Spectra and Molecular Structure IV, Constants of Diatomic Molecules," Van Nostrand, New York, 1979.
3. O. APPELBLAD, R. F. BARROW, AND R. D. VERMA, *J. Phys. B* **1**, 274-282 (1968).
4. R. W. MARTIN AND A. J. MERER, *Canad. J. Phys.* **51**, 634-643 (1973).
5. Y. HOUBRECHTS, I. DUBOIS, AND H. BREDOHL, *J. Phys. B* **12**, 2137-2141 (1979).
6. Y. HOUBRECHTS, I. DUBOIS, AND H. BREDOHL, *J. Phys. B* **13**, 3369-3373 (1980).
7. Y. HOUBRECHTS, I. DUBOIS, AND H. BREDOHL, *J. Phys. B* **15**, 603-611 (1982).
8. Y. HOUBRECHTS, I. DUBOIS, AND H. BREDOHL, *J. Phys. B* **15**, 4551-4560 (1982).
9. M. TANIMOTO, S. SAITO, Y. ENDO, AND E. HIROTA, *J. Mol. Spectrosc.* **100**, 205-211 (1983).
10. Y. AKIYAMA, K. TANAKA, AND T. TANAKA, *Chem. Phys. Lett.* **155**, 15-20 (1989).
11. G. GUELACHVILI AND K. NARAHARI RAO, "Handbook of Infrared Standards," Academic Press, New York, 1986.
12. E. HILL AND J. H. VAN VLECK, *Phys. Rev.* **32**, 250-272 (1928).
13. R. S. MULLIKEN AND A. CHRISTY, *Phys. Rev.* **38**, 87-119 (1931).
14. G. M. ALMY AND R. B. HORSFALL, *Phys. Rev.* **51**, 491-500 (1937).
15. G. C. DOUSMANIS, T. M. SANDERS, JR., AND C. H. TOWNES, *Phys. Rev.* **100**, 1735-1754 (1955).
16. L. VESETH, *J. Mol. Spectrosc.* **38**, 228-242 (1971).
17. M. MIZUSHIMA, *Phys. Rev. A* **5**, 143-157 (1972).
18. R. N. ZARE, A. L. SCHMELTEKOPF, W. J. HARROP, AND D. L. ALBRITTON, *J. Mol. Spectrosc.* **46**, 37-66 (1973).
19. E. HIROTA, "High-Resolution Spectroscopy of Transient Molecules," Springer-Verlag, Berlin/New York, 1985.
20. I. KOPP AND J. T. HOUGEN, *Canad. J. Phys.* **45**, 2581-2596 (1967).
21. J. M. BROWN, J. T. HOUGEN, K. P. HUBER, J. W. C. JOHNS, I. KOPP, H. LEFEBVRE-BRION, A. J. MERER, D. A. RAMSAY, J. ROSTAS, AND R. N. ZARE, *J. Mol. Spectrosc.* **55**, 500-503 (1975).
22. J. M. BROWN AND J. K. G. WATSON, *J. Mol. Spectrosc.* **65**, 65-74 (1977).
23. Y. ENDO, S. SAITO, AND E. HIROTA, *J. Mol. Spectrosc.* **92**, 443-450 (1982).
24. K. KAWAGUCHI, S. SAITO, AND E. HIROTA, *J. Chem. Phys.* **79**, 629-634 (1983).
25. H. SHOJI, T. TANAKA, AND E. HIROTA, *J. Mol. Spectrosc.* **47**, 268-274 (1973).
26. K. KAWAGUCHI, C. YAMADA, Y. HAMADA, AND E. HIROTA, *J. Mol. Spectrosc.* **86**, 136-142 (1981).
27. J. L. WANG, C. N. KRISHNAN, AND J. L. MARGRAVE, *J. Mol. Spectrosc.* **48**, 346-353 (1973).